Available online at www.sciencedirect.com
SCIENCE DIRECT
Scripta Materialia 54 (2006) 513–520
Scripta MATERIALIA
www.actamat-journals.com

Amorphous metal foams

A.H. Brothers, D.C. Dunand *

Department of Materials Science and Engineering, Northwestern University, Cook Hall, 2220 Campus Drive, Evanston, IL 60208, USA

Received 17 February 2005; received in revised form 3 June 2005; accepted 24 October 2005
Available online 14 November 2005

Abstract

As recently demonstrated, amorphous metal foams are highly ductile in compression, and thus offer attractive compromises in mechanical and physical properties between crystalline metallic and ceramic foams. Challenges associated with fabrication of amorphous metal foams are critically assessed in the context of current and future processing methods, and conclusions are drawn regarding the properties and future applications of ductile amorphous metal foams.

Keywords: Metallic glasses; Amorphous metals; Foams; Foaming; Processing

1. Introduction

Crystalline metallic foams, most commonly made from aluminum alloys, are known for their high density-compensated mechanical properties in compression, bending and torsion (including excellent plastic energy dissipation) and useful thermal and acoustic properties [1–3]. Metallic foams and foam sandwich structures enjoy increasing use, e.g., as lightweight structural members, impact/blast mitigators, fluid filters, catalytic supports, and biomedical implants. Similarly, bulk amorphous metals (those with maximum casting dimensions of at least one millimeter) are seeing increased use in applications such as sporting goods and cellular telephone housings, because of their exceptionally high strength and elastic strains, high wear and corrosion resistance, and excellent processability due to low melting temperatures and superplastic-like flow at high temperatures [4–6].

Metallic foams suffer from a familiar trade-off between strength and processability: aluminum-based foams can be easily fabricated by various processes but have mechanical properties limited by those of their base alloys, while foams made from stronger crystalline alloys generally require higher-temperature and/or more difficult processing methods. For bulk amorphous metals, the major limitations are poor ductility in uniaxial deformation (typically ~0% in tension and <0.5% in compression [6]) and high processing costs [7], the latter also being a problem for metallic foams [8]. Some key limitations of each material class might be addressed through creation of amorphous metal foams (AMF), which combine some of their respective key advantages (e.g., the energy absorption/high compressive plastic strain of foams and the high strength and modest processing temperatures of amorphous metals) into a promising new alternative.

In this paper, challenges presented by AMF processing are analyzed and current and future solutions discussed. Furthermore, the mechanical properties of available AMF are summarized, and future applications are proposed, based on available data and knowledge taken from amorphous metals and crystalline metallic foams.

2. Processing of amorphous metal foams

2.1. Processing challenges

Several difficulties in modern foaming methods continue to complicate the production and uptake of metallic foams, e.g., pore size control, macroscopic uniformity and isotropy,

* Corresponding author. Tel.: +1 847 491 5370; fax: +1 847 491 7820.
E-mail address: dunand@northwestern.edu (D.C. Dunand).

1359-6462/$ - see front matter
doi:10.1016/j.scriptamat.2005.10.048

and cost effectiveness, as thoroughly reviewed elsewhere (see Ashby et al. [1] and sources therein). The focus of the present discussion will instead be considerations unique to foaming of amorphous metals which lead to additional complications outside those inherent to all metal foams. We believe that the two most important of these considerations are compositional accuracy and cooling rate requirements, and these are discussed in detail below.

Optimal bulk amorphous alloys are mostly found near deep eutectic features in phase space, and are therefore usually surrounded by steep liquidus surfaces [4–6]. Deviation from the optimal composition due to reactions with external phases (e.g., crucible materials, or impurities from low-quality components or processing environments) is therefore usually accompanied by rapid increases in the temperature at which stable crystalline phases can appear during solidification, complicating or even making impossible the step of cooling through the glass transition without significant crystallization. Very pronounced deterioration occurs when impurities (most importantly oxygen [9,10]) trigger formation of refractory solid phases in the melt whose crystal structure, wetting/dispersion characteristics, or effect on local ordering cause them to act as heterogeneous nucleants for the native crystalline phases of the alloy [9–11].

Compositional and purity requirements are readily addressed (at some expense) through clean processing techniques, but impose limits on which processing equipment and external phases are 'compatible' with a particular alloy, as exemplified by results from amorphous metal–matrix composites [12–14]. Foaming, like composites processing, often entails introduction of a substantial fraction of external phases, e.g., blowing agents or solid placeholders, in order to achieve porosity. Successful AMF processing methods must therefore ensure compatibility between the host alloy and any foreign phases required during foaming. In addition, most foaming techniques seek to produce small, uniform pore size in order to ensure isotropic and statistically-reliable foam properties (data from conventional metallic foams show consistency only when the pore size is 7–10 times smaller than the minimum foam dimension [1]). As a result, finely-dispersed blowing agents and placeholders are often desirable, at the cost of high contact areas with the alloy and proportionally more severe chemical interactions. A compromise must thus be drawn between desired AMF property uniformity and degraded glass-forming ability. Promising work on the effects of low-concentration scavengers (e.g., Sc [9] and Y [9,15]) should however allow more favorable compromises to be drawn in the future, by improving the robustness of glass-forming alloys in the presence of fine external phases.

The second unique limitation of bulk amorphous metals is the need for high cooling rates between the molten state and glass transition to suppress crystallization, on the order of 1–10 K/s (though exceptional alloys exist with even lower critical cooling rates) [4–6]. Cooling rate requirements exacerbate the need for fine porosity by placing limits on maximum achievable foam dimensions, and thereby on maximum allowable pore size, for foams processed in the liquid state. The severity of these limitations can be estimated using data compiled by Ashby et al. from conventional metal foams [1]. These data suggest that thermal conductivity λ for metallic foams scales roughly as $(\rho/\rho_s)^{1.7}$ (with ρ and ρ_s the foamed and monolithic densities, respectively), while specific heat c_p is independent of density. Thus thermal diffusivity $\alpha = \lambda/\rho c_p$ scales as $(\rho/\rho_s)^{0.7}$. The characteristic thermal diffusion distance, which is proportional to $(\alpha t)^{1/2}$ (where t is the duration of the quench), then scales as $(\rho/\rho_s)^{0.35}$ because t is defined by the temperature interval of the quench and critical cooling rate of the alloy, both being constants for any particular alloy in the absence of contamination. This characteristic distance defines the thickness of material through which a thermal wave-front may pass during a quench from the molten state, and is thereby directly related to the maximum castable dimension of the amorphous material; this dimension should then scale roughly as $(\rho/\rho_s)^{0.35}$. According to this reasoning, an AMF of relative density 30% could be cast from the liquid state with dimensions roughly 66% those of the monolithic alloy. Modern bulk amorphous alloys are regularly vitrified in dimensions of 10–100 mm [6], suggesting maximum foam dimensions in the range of 6.6–66 mm. Applying the statistical criterion above, maximum pore sizes must in turn fall in the range of 0.66–9.4 mm, well within the capabilities of existing foaming processes. Repeating the analysis for an AMF of relative density 10% gives similar foam dimensions (4.5–45 mm) and pore sizes (0.45–6.4 mm), because of the relatively low sensitivity of the diffusion distance to density. This analysis also highlights the fact that successful processes for low-density AMF must simultaneously ensure fine porosity, a restriction unique to AMF and in conflict with the need to avoid alloy contamination caused by incorporating high volume fractions of fine pore-forming phases.

The above treatment, though far from exact, motivates the important conclusion that limitations incurred by rapid solidification are not stringent enough to prevent the practical development of AMF, even in methods where the alloy is fully-foamed before quenching from a molten state. This is important because many liquid-state foaming methods, for example casting around soluble/burnable/hollow placeholders or into investment molds, as well as four of the five methods already demonstrated for AMF, take this approach. It is also important because it represents the "worst-case scenario" from the standpoint of meeting cooling-rate requirements within the glass-forming phase; as discussed below, many foam processing methods, properly adapted to amorphous metals, might avoid the need to quench poorly-conducting fully-foamed melts. Combined with continuing improvements in glass-forming alloys, which already boast more than a thousand-fold increase in maximum casting dimensions over the last forty years [5], these adaptations should eventually render cooling rate a secondary consideration in AMF processing.

2.2. Current processing methods

The search for AMF processing methods began with the work of Apfel and Qiu [16,17], who proposed foaming amorphous metals using an approach previously used with glassy polymers. In this method, foams are created by rapid vaporization during pressure-quenching of mixtures of glass-forming melts with insoluble, nonreactive, volatile foaming agents. The rapid cooling needed to suppress crystallization is accomplished naturally as the latent heat of evaporation of the volatile agent is extracted from the melt. The method has not, however, been demonstrated for amorphous metals, likely because no volatile but nonreactive foaming agents have been identified.

The first successful method was reported in 2003, nearly a decade after the work of Apfel and Qiu, and is based on expansion of water vapor bubbles formed during decomposition of hydrated B_2O_3 flux particles in a $Pd_{43}Cu_{27}Ni_{10}P_{20}$ melt [18]. Reported densities were as low as 1.4 g/cm^3 ($\rho/\rho_s = 16\%$), with closed pores of 200–1000 μm size. This process was later modified so that only a small fraction (15 vol.%) of small pores (75 μm) was introduced at high temperature, while expansion to pore sizes and fractions comparable to the simpler method was accomplished at lower temperature [19]. A similar alloy, $Pd_{42.5}Cu_{30}Ni_{7.5}P_{20}$, was also foamed by quenching mixtures of the glass-forming melt and NaCl granules, followed by dissolution of the NaCl placeholder in water [20]. Using this latter method, densities as low as 3.3 g/cm^3 ($\rho/\rho_s = 35\%$) were produced, with small open cells about 125–250 μm in size. In 2004, the same group reported an additional method for foaming Pd-based amorphous alloys, where hydrogen was dissolved into the melt at high pressure and then precipitated and trapped as bubbles during simultaneous pressure and temperature quenching [21], an approach reminiscent of hydrogen-metal eutectic methods used to produce 'gasar' or 'lotus-type' foam structures in crystalline metals [22]. Using this method, densities of 3.4 g/cm^3 ($\rho/\rho_s = 36\%$) were achieved, with closed pores averaging 200 μm in size.

Earlier in 2004, closed-cell foam had been processed from the alloy $Zr_{57}Nb_5Cu_{15.4}Ni_{12.6}Al_{10}$ (Vit106) by infiltration of beds of hollow carbon microspheres, yielding closed-cell 'syntactic' foam with net density 3.4 g/cm^3 ($\rho/\rho_s = 50\%$) and very small pores (25–50 μm) [23]. Porosity was reportedly introduced into a closely-related alloy by entrainment of gas into the melt during rapid convection, but no evidence was provided of porosities exceeding 10 vol.% ($\rho/\rho_s = 90\%$) [19]. Beginning in early 2005, a second complete method was described for Vit106, involving infiltration of sintered BaF_2 placeholders followed by salt leaching in acid baths [24,25]. Densities of 1.0–1.9 g/cm^3 ($\rho/\rho_s = 14$–28%), with open pores as small as ~150 μm were reported [26].

Images showing the structures of available AMF are provided in Fig. 1. The figure illustrates important similarities and contrasts between pore structures: gas-generated and syntactic foaming produce spheroidal, closed pores, while salt methods produce angular, open pores. In addition, every method yields pore sizes in the range of hundreds of microns or less, within the critical range discussed in the previous section. Sample diameters of at least 5 mm were achieved in all cases, even using the Be-free commercial Zr-based alloy Vit106 with a critical bulk casting thickness around 10 mm (in that case, high relative diameters of 7 mm were reported [14]), and none of the reports explicitly names a maximum diameter beyond which crystallization was evident.

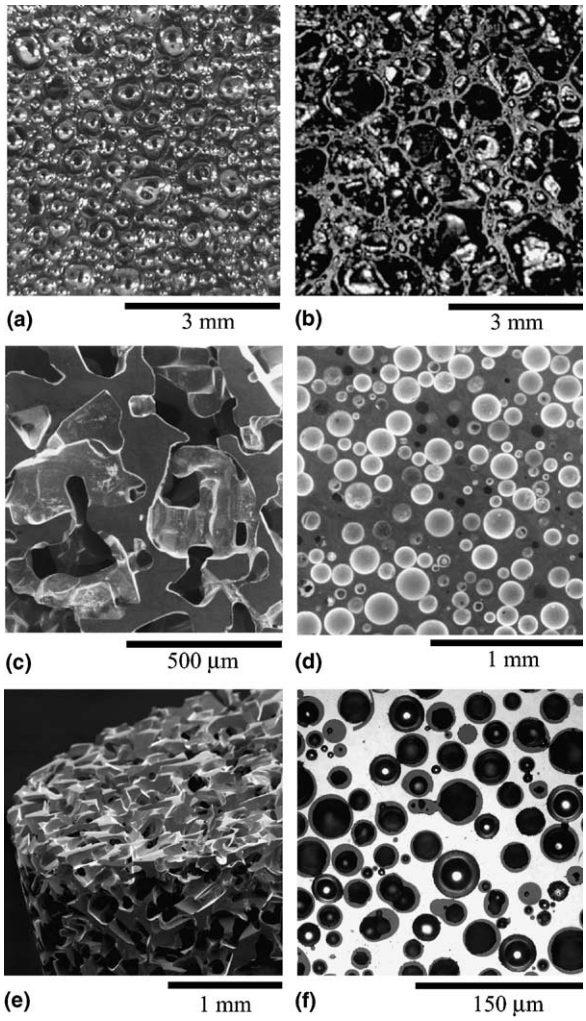

Fig. 1. Amorphous metal foams reported in the literature: (a) Pd-based foam made using a gas-generating flux additive ($\rho/\rho_s = 24\%$) [18], (b) Pd-based foam made by entrapping gas in the melt and then expanding it in the supercooled-liquid state ($\rho/\rho_s = 15\%$) [19], (c) Pd-based foam made by quenching a mixture of the molten glass-forming alloy and leachable NaCl granules ($\rho/\rho_s = 35\%$) [20], (d) Pd-based foam made by precipitation of dissolved hydrogen gas during cooling. The relative density of this foam was not listed, but is likely to lie in the range $\rho/\rho_s = 54$–58%) [21], (e) Zr-based foam made by casting into a bed of sintered, leachable BaF_2 particles ($\rho/\rho_s = 22\%$) [24] and (f) Zr-based foam made by casting into a bed of hollow carbon microspheres ($\rho/\rho_s = 50\%$) [23].

2.3. Future processing methods

A unifying feature of the methods reported to date is their use of the liquid state as a vehicle for foaming. This

is a natural reflection of the fact that the high viscosity of glass-forming melts [4] improves foam stability by slowing deleterious drainage, coarsening, and sedimentation processes; the equilibrium viscosity of a typical bulk glass-forming melt at its liquidus is roughly three orders of magnitude higher than that of a typical pure metallic melt, and higher still in the supercooled-liquid region [18]. Such high viscosities may allow glass-forming alloys to be foamed in the liquid state without the ceramic thickening additives used with crystalline metals, simplifying processing [1]. Use of the liquid state also reflects the fact that foaming above the liquidus temperature, where crystallization is thermodynamically forbidden, affords nearly unlimited (i.e., only contamination-limited) processing windows. Still, several promising liquid-state approaches have not yet been successfully applied to amorphous metals, for example direct gas injection (e.g., through impellers, nozzles, or porous crucible walls) [27] or entrainment of cover gases during rapid agitation [28], though these methods may benefit from simplicity and low cost (and though, as mentioned previously, a direct gas entrapment approach was partially implemented with a Zr-based amorphous alloy [19]). Other methods, e.g., replication of sacrificial polymer foams using investment casting in refractory molds, have enjoyed limited study for amorphous metals and may prove useful in future work [29].

It has already been suggested above that the effective thermal conductivity of foamed melts is sufficient to allow vitrification of liquid-state foams in useful, if limited, dimensions. Since thermal conductivity is still diminished by porosity, however, alternative foaming methods can be imagined where quenching occurs at the strut level, as opposed to the foam level. In the simplest case, open-celled foams could be quenched directly into inert quenchants, allowing each strut to cool individually. It is unlikely that conventional water and oil-based quenchants could be used in this way without severe losses of glass-forming ability, but the much-improved cooling rates associated with strut-level quenching may allow less effective but more inert quenchants (e.g., inert gas) to be substituted, at least for lower-melting and/or less-reactive alloys. As a more ambitious example, a modified investment casting method can be imagined in which the sacrificial open-cell polymer foam is dip-coated in ceramic slurry rather than fully invested, such that the mold after drying consists of a thin ceramic shell around each strut instead of a full negative pattern. High-temperature firing to remove the polymer results in a ceramic foam with open cells and hollow struts, which are subsequently filled with a liquid glass-forming alloy. The open structure of this ceramic-coated liquid foam then allows the quenchant to cool the alloy at the strut level, affording much higher and more uniform cooling rates than would be possible using solid investment molds. Similarly, hollow lattice-truss structures such as those developed by Queheillalt and Wadley could be infiltrated and quenched [30]. In any such method, relatively large pore size would be required in order to assure uniform penetration and convection of the quenchant, especially if the quenchant vaporizes on exposure to the struts; larger pore size would be acceptable, however, because decoupling the foaming and vitrification steps in this way eliminates foam dimensional limitations.

A simpler and more elegant way to decouple foaming and vitrification is to foam only in the supercooled-liquid (SCL) region, between the glass transition and characteristic crystallization temperature of the base alloy. The approach applied by Schroers et al. [19] is an example of a hybrid processing method employing both the liquid and SCL states. In this process, pores (e.g., pressurized inert gas) or pore-forming phases (e.g., hydrated B_2O_3) are dispersed in small fractions within a molten glass-former, minimizing difficulties associated with contamination and loss of thermal conductivity prior to quenching. After quenching to achieve a fully amorphous structure, the resulting 'prefoam' materials are then reheated into the SCL region, where foaming by gas expansion can occur within a time window allowed by the crystallization kinetics of the alloy. The SCL region is typically 20–135 K in width, depending on the alloy, heating rate and thermal history, [6] and always lies below the nose of the crystallization TTT curve. For this reason, cooling rate limitations (and therefore dimensional limitations) are all but eliminated when cooling from the SCL state, and processing windows of up to 30 min would become available for foaming of the best-known glass-formers, due to very sluggish crystallization kinetics in the supercooled melt [31,32]. Within the SCL region, furthermore, viscosity typically lies in the range of 10^7–10^{12} Pa s, implying proportionally sluggish pore coarsening and collapse kinetics [19]. Such methods show great promise for AMF because they permit casting of prefoam ingots having nearly the same dimensions available to the pore-free alloys, and because it is possible to subsequently place prefoam materials within net-shaped molds to determine their final shape after expansion, as is often done with Al-based foams [33]. The success of all such methods will be determined by the relationship between the timescales of pore expansion, pore collapse, and alloy crystallization within the SCL region; better glass-formers typically have larger temperature and time windows available before crystallization occurs, and thus greater chances of success using this strategy.

Introducing pores or pore-forming phases above the liquidus, as described by Schroers et al. [19], is one approach combining liquid-state and SCL foaming. Another approach relying solely on SCL-state foaming would consist of blending pore-formers with amorphous metal powders, followed by consolidation (and/or expansion) of the powder mixture in the supercooled-liquid region. Alternatively, amorphous metal powders could be consolidated in the presence of a high-pressure inert gas, forming individual pores which are then expanded in the SCL temperature range, similar to crystalline titanium foams [34]. Reports offer evidence that amorphous metal

powders can be consolidated in the SCL region with little or no loss of strength using hot pressing [32], warm rolling [35], and conventional area reduction [31,36] or equal-channel angular [37] warm extrusion techniques; partial consolidation (to relative densities ca. 75%) of amorphous powders has been reported and could be used to augment porosity generated by any such processes (albeit with some additional loss in strength) [38]. It is easy to envision incorporation of placeholders into these consolidated compacts, providing a natural method for making low-density foams with low processing temperatures. Many existing placeholders used for conventional metals (e.g., urea, salts, or hollow spheres) might then be extended to AMF processing, for example using Mg-based amorphous alloys, which have been consolidated at temperatures as low as 373 K [39]. For gas-generating pore-formers, SCL-state processing would be more difficult, as adequate expansion would depend on achieving consolidation prior to release of the gas, for example by using low temperature and heavy deformation to consolidate, followed by higher temperature and vacuum to promote expansion. Unlike dispersion in the liquid state, these methods would require no high-temperature steps (except perhaps the initial step of making amorphous powders), allowing much greater flexibility in the selection of equipment and pore-forming phases while still eliminating dimensional limitations. Another example of SCL-state foaming would be consolidation of hollow spheres, as demonstrated for crystalline metals [40]. Thin-walled hollow amorphous metal spheres, fabricated and vitrified using concentric-nozzle spraying, would be heated into the SCL region under applied stress, causing them to deform and bond while retaining their internal porosity. If this consolidation could be achieved on shorter timescales than crystallization, the resulting structures could achieve very low density and large dimensions using a wide range of glass-forming alloys, with no need for introduction of external phases.

True solid-state processing methods, those whose working temperatures remain entirely below the glass transition temperature, can also be envisioned. Though it would be natural to suggest the use of powder metallurgical techniques in this context as well, no literature seems to exist documenting successful consolidation of amorphous powders below the glass transition, probably due to the very high flow stresses of amorphous metals at low temperature and, possibly, the presence of bond-inhibiting oxide films on the powder surfaces [36]; as such, it is likely that most powder methods will instead fall into the category of SCL-state processing like those described above. Nonetheless, two true solid-state methods are conceivable: firstly, honeycomb structures fabricated from amorphous metal ribbons by mechanical bonding (e.g. stamping); and second, textile structures woven from amorphous metal wires. Both methods would enjoy the advantage of completely decoupling the vitrification and 'foaming' steps, eliminating dimensional and alloy limitations, but would also be limited in terms of available architecture and properties, and as noted above, it is not yet clear that good bonding can be achieved without heating.

The final set of potential AMF processing methods are vapor-state methods, used commonly, for example, in processing of crystalline Ni-based foams [1]. Vapor-state processing through chemical or physical vapor deposition onto sacrificial substrates may find application to AMF as well; such methods should be particularly appropriate for the many chemically-simple glass-formers having critical cooling rates too high for liquid-state processing, as the effective cooling rates associated with vapor processes are substantially higher than those possible in the bulk. For more sophisticated, higher-order amorphous alloy systems, ensuring compositional accuracy and uniformity may prove difficult; in any case, vapor-state processing would be unnecessary for these systems, as their critical cooling rates are typically low enough to allow simpler foaming methods to be applied.

Though it was natural, in the interest of simplicity, to first develop foaming techniques using pure glass-forming alloys, amorphous metal–matrix composites could also be used as starting points for any of the methods above, with the exception of vapor-state methods. Such composites, consisting of amorphous metallic matrices containing metallic and ceramic reinforcements with continuous or discontinuous geometries [12–14], are known to have much greater intrinsic ductility than their single-phase counterparts. Though most such composites exhibit reinforcements added ex-situ by conventional melt-infiltration techniques, others can be precipitated in-situ during alloying and casting steps, simplifying processing. Though at present these 'β-phase' composites mostly contain refractory crystalline Ta [41] or Nb [42] phases, development of similar composite systems for lower-melting glass-forming systems with lower-melting reinforcements may allow both foaming and ductilization to be accomplished in a single melting step. In certain cases, simple heat treatments can also induce beneficial nanocrystallization in amorphous metals, and identical treatments might also be applied to AMF. Irrespective of the method of their introduction, second phases could serve as a means of intrinsic ductilization for AMF, rendering extrinsic ductilization by control over foam architecture (discussed in the next section) less critical. This is similar to the intrinsic and extrinsic approaches applied to the ductilization of other brittle materials, e.g. ceramics and intermetallics. In each application, improved ductility and damage tolerance would need to be weighed against side effects such as additional processing difficulty or diminished corrosion resistance (due to new grain or interphase boundaries, and/or galvanic interaction between phases).

Finally, it is important to note that conventional metal foams are widely used as cores in sandwich structures, because such structures offer substantial improvements to mechanical properties and greater flexibility in forming, finishing, and joining operations, with minimal impact to overall density [1,43]. The same would likely be true for

AMF, though difficulties in diffusion bonding AMF cores to faceplates (without inducing crystallization) may necessitate development of integral processing methods where facing layers are formed or bonded before or during foaming, for example by roll-cladding of facing materials onto powder compacts prior to SCL-state foaming. The high specific strength and excellent wear- and corrosion resistance of amorphous metals, along with their enhanced plasticity in confined deformation modes like rolling [44] make them natural choices for SCL-state facings, especially if integral methods are developed. Crystalline metallic facings may be considered due to their high uniaxial ductility, at the cost of added processing difficulty and increased likelihood of inducing brittle crystalline phases near the core-facing interface.

3. Mechanical properties of amorphous metal foams

If AMF were to suffer the same lack of compressive ductility as monolithic amorphous metals, their high cost would certainly render them inferior to ceramic foams, which themselves are rarely useful in nonstatic load-bearing applications [2]. Pores in AMF may however confine shear band propagation and increase shear band densities by blocking the small number of bands normally responsible for compressive failure in monolithic bulk amorphous samples, in much the same way that reinforcing metallic or ceramic phases enhance compressive ductility in amorphous metal–matrix composites [45,46]. Thin amorphous metal ribbons and wires, which share much in common with the features present within most cellular amorphous metals, show high bending ductility [47]. Surface strain to failure in sub-millimeter Zr-based ribbons and wires lies in the range 5–200%, for example, and these can often be bent in half without fracture, suggesting an additional source of ductility for AMF. Though the few existing studies on the mechanical properties of AMF pertain specifically to uniaxial compression, ductilizing effects in AMF have already been convincingly established, as discussed in detail below.

Mechanical properties have been reported by Wada and Inoue for Pd-based AMF with relative densities between 36% and 64%, made by the hydrogen entrapment method [21]. The yield strength of these foams increases from 220 to 500 MPa in this density range, followed by gradually-declining serrated flow stresses (Fig. 2a). Final failure occurs at strains of 12–16%, well in excess of monolithic amorphous alloys. Interpretation of these values cannot be performed using classical cellular metal models which are valid for foams with densities below 30%, due to their reliance on beam theories [1,2]. Then, improvements in ductility through introduction of low (<70%) porosity levels are probably best rationalized in terms of unstable shear band arrest, an approach mostly used in the context of amorphous metal–matrix composites [45,46]. Mechanical properties for higher-porosity, open-cell AMF, which benefit from arrest mechanisms as well as the enhanced ductility associated with thin elongated struts deformed in bending, have been reported by Brothers and Dunand [25,26]. Yield strength was shown to increase from 16 to 34 MPa as relative density increased from 18% to 28%, while high strains, typically in excess of 80%, were achieved without macroscopic sample fracture. Unlike their higher-density counterparts, these foams exhibited stress–strain curves (Fig. 2a) mostly characteristic of conventional ductile crystalline metal foams: no stress drop at yield, an extended plateau region, and gradual densification at high strain. However, the same serrations seen in the stress–

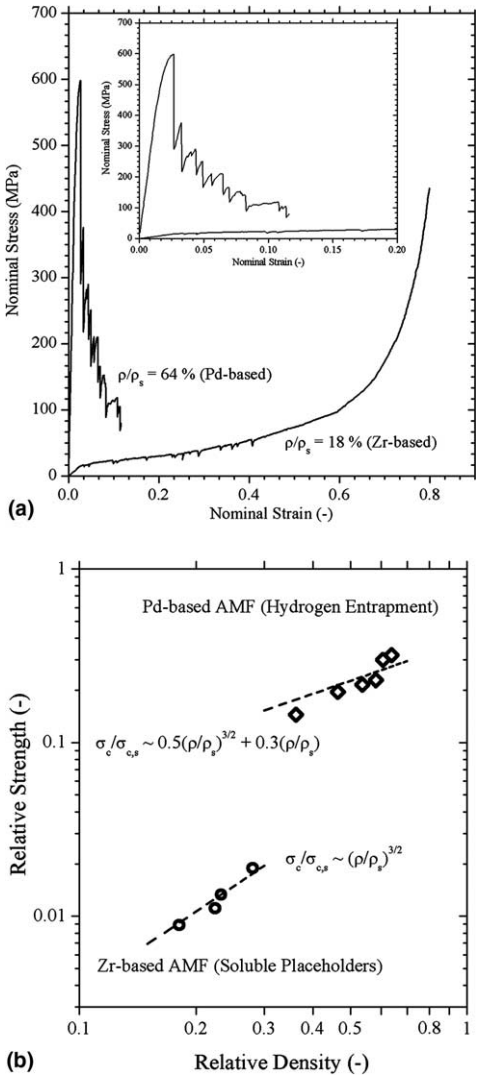

Fig. 2. Published compressive mechanical properties of amorphous metal foams: (a) Nominal stress strain curves for high-density ($\rho/\rho_s = 64\%$) Pd-based foam with closed porosity [21] and low-density ($\rho/\rho_s = 18\%$) Zr-based foam with open porosity [26]. The former shows high strength but comparatively small ductility, while the latter shows classical ductile metal foam behavior at much lower stresses and (b) foam yield strength (normalized to the compressive strength of the corresponding monolithic alloy, $\sigma_{c,s}$) as a function of foam relative density, for open-cell Zr-based foams with high porosity, and for closed-cell Pd-based foams with low porosity. Best fits using semi-empirical scaling laws described by Ashby et al. [Ref. [1], Table 4.2] for opened- and closed-cell metal foams are also shown.

strain curves of higher-density AMF described above were still apparent, reflecting the fact that in a stochastic foam structure some struts will always fail axially (in a brittle manner for AMF) due to insufficient aspect ratio and/or local loading conditions unsuitable for bending. Acoustic emission studies into serrations in the low-density AMF indicate that they result from the sudden localization of microfracture damage accumulated slowly during compression [48].

Data for normalized yield strength of both Zr- and Pd-based AMF are summarized in Fig. 2b. In the interest of consistency with similar data from aluminum foams, compressive strength is used to normalize these data; it has been pointed out [25,26], however, that this is not strictly correct for materials having tensile-compressive asymmetry, such as amorphous metals [49]. Examination of Fig. 2b suggests that the transition between the extreme behaviors of Fig. 2a may occur near a relative density of 30%. This transition seems to consist of decreased strength and increased ductility, and therefore likely represents an underlying transition between two deformation regimes dominated, respectively, by uniaxial and (less mechanically-efficient) bending deformation modes. It is likely, however, that a portion of the observed strength loss arises from differences in the foam architectures: the Zr-based foams are open-cell, which are typically slightly weaker than closed-cell foams of similar density, and also have highly angular pores, giving higher local stress concentrations, unlike the closed-cell Pd-based foams exhibiting spherical pores. More significant is the large change in foam ductility, reflecting the abrupt change in ductility associated with bending of slender amorphous metal features. This interpretation is supported by visual observations, which show large and relatively sparse cracks and shear bands in a compressed high-density foam [21] but evidence of extensive and well-distributed ductile plastic hinging in a low-density foam [25,26].

Although further investigation of the details of deformation in AMF is certainly needed, these recent reports clearly indicate that ductility, as gauged by macroscopic compressive failure strain, is dramatically higher for AMF than for monolithic amorphous metals, even in the absence of intrinsic ductilizing factors like ductile reinforcements. This critical result motivates evaluation of the potential applications of AMF, as described in the next section.

4. Applications for amorphous metal foams/sandwiches

Applications for ductile AMF (most probably as cores in sandwich structures) may be expected to parallel those of conventional metal foams, with differences reflecting the advantages of the amorphous state. First and most obvious among these is a substantial increase in achievable specific strength, due to the high specific strength of amorphous metals: with modest densities of 2–9 g/cm^3 [50,51], compressive strength values are in the range of 0.5–5 GPa in compression, slightly lower in tension [5]. The resulting high strength/density ratios will expand the envelope of foams for specific-strength-limited designs, e.g., static beams, columns or plates (structural members), rotating disks (flywheels), shells (pressure vessels) and rotating drums (centrifuges) [1]. Also, the high strength/stiffness ratio (i.e. high elastic strain) of amorphous metals should make certain AMF applications, such as elastic hinges and compression gaskets, optimal [1].

Ductile AMF show particular promise for impact mitigation applications where available metal foams lack the necessary strength. Energy dissipation per unit volume, for a given densification strain (which for ductile foams is a function primarily of porosity and architecture), scales near-linearly with strength. It should be noted, however, that increases in strength, while advantageous in conventional structural applications, are not always desirable for impact mitigation applications. Stronger foams dissipate more energy but also transmit larger stresses, such that AMF should be superior for mitigating impacts to vehicles or structures, but may transmit unacceptably large forces to delicate objects or human beings [1].

Another important limitation facing the use of AMF in structural roles is service temperature. Amorphous metals experience relaxation near the glass transition, leading in many cases to much reduced toughness, and crystallize ca. 20–135 K above the glass transition, depending on the specific alloy, heating rate and thermal history [6]. These effects will limit extended service to temperatures well below the glass transition, which is typically in the range of 300–750 K [6]. As with crystalline alloys, increased service temperatures in AMF will require increased processing temperatures, exacerbating processing difficulty and cost.

As compared to crystalline metal foams, AMF should have improved corrosion resistance due to their lack of grain boundaries, dislocations, and other sites of preferential attack [52,53]. Corrosion resistance is useful in all structural applications, but in the case of AMF would be advantageous in other foam applications as well, for example in electrodes, filters, or catalyst supports. Another promising application requiring high specific strength alongside corrosion- and wear resistance is orthopedic biomaterials, where open-cell AMF may compete with crystalline Ti-based foams currently used for bone replacements [34,54]. Though the supporting literature is less complete for amorphous metals than for titanium and other well-established biomedical alloys, several reports show promising corrosion properties for amorphous metals in simulated biological fluids, one of the key requirements of biocompatibility [55–57]. Also, most amorphous metals are nonmagnetic, facilitating post-operative imaging and evaluation as compared to modern Fe- and Co-based prosthetic implants. High strength would allow smaller, less intrusive AMF implants, while comparatively modest elastic moduli (50–150 GPa for monolithic bulk amorphous metals, corresponding to high elastic limits of 2% [6]) would allow porous implant stiffness to be more easily matched with host bone tissues. Stiffness matching is

considered an essential part of alleviating stress-shielding complications in bone replacements [58].

5. Summary and outlook

The unique challenges faced in development and production of amorphous metal foams parallel those faced by amorphous metals in general, i.e., the need to ensure purity and rapid cooling while controlling costs. Progress in the identification and understanding of new glass-forming systems with still higher robustness against contaminants and slow cooling, which is currently the subject of intensive research, should lead to equivalent progress in AMF. In the past few years, foaming methods adapted to the requirements of available glass-forming alloys have already been created and studied. Using these methods, the critical existence of compressive ductility in AMF has been demonstrated, and the engineering potential of this novel class of materials established. Though much research remains to be done before the unique properties of AMF can be fully realized, a number of applications can already be foreseen, ranging from catalytic substrates to bone replacement materials to high-strength impact absorbers and vehicle/structure armor.

Acknowledgements

The authors are grateful for financial support through the DARPA Structural Amorphous Metals Program (ARO Contract No. DAAD 19-01-1-0525), managed by the Caltech Center for Structural Amorphous Metals.

References

[1] Ashby MF, Evans AG, Fleck NA, Gibson LJ, Hutchinson JW, Wadley HNG. Metal foams: a design guide. Boston (MA): Butterworth-Heinemann; 2000.
[2] Gibson LJ, Ashby MF. Cellular solids: structure and properties. 2nd ed. Cambridge: Cambridge University Press; 1997.
[3] Banhart J. Prog Mater Sci 2001;46:559.
[4] Johnson WL. Mater Sci Forum 1996;225:35.
[5] Inoue A. Acta Mater 2000;48:279.
[6] Wang WH, Dong C, Shek CH. Mater Sci Eng 2004;R44:45.
[7] Salimon AI, Ashby MF, Brechet Y, Greer AL. Mater Sci Eng A 2004;375–77:385.
[8] Maine E, Ashby MF. Adv Eng Mater 2000;2:205.
[9] Kundig AA, Lepori D, Perry AJ, Rossmann S, Blatter A, Dommann A, Uggowitzer PJ. Mater Trans 2002;43:3206.
[10] Liu CT, Chisholm MF, Miller MK. Intermetallics 2002;10:1105.
[11] de Oliveira MF, Botta FWJ, Kaufman MJ, Kiminami CS. J Non-Cryst Sol 2002;304:51.
[12] Dandliker RB, Conner RD, Johnson WL. J Mater Res 1998;13:2896.
[13] Choi-Yim H, Busch R, Koster U, Johnson WL. Acta Mater 1999;47:2455.
[14] Choi-Yim H, Conner RD, Szuecs F, Johnson WL. Acta Mater 2002;50:2737.
[15] Lu ZP, Liu CT, Porter WD. Appl Phys Lett 2003;83:2581.
[16] Qiu N, Apfel RE. Rev Sci Instrum 1995;66:3337.
[17] Apfel RE, Qiu N. J Mater Res 1996;11:2916.
[18] Schroers J, Veazey C, Johnson WL. Appl Phys Lett 2003;82:370.
[19] Schroers J, Veazey C, Demetriou MD, Johnson WL. J Appl Phys 2004;96:7723.
[20] Wada T, Inoue A. Mater Trans 2003;44:2228.
[21] Wada T, Inoue A. Mater Trans 2004;45:2761.
[22] Nakajima H, Ikeda T, Hyun SK. Adv Eng Mater 2004;6:377.
[23] Brothers AH, Dunand DC. Appl Phys Lett 2004;84:1108.
[24] Brothers AH, Scheunemann R, DeFouw JD, Dunand DC. Scripta Mater 2005;52:335.
[25] Brothers AH, Dunand DC. Adv Mater 2005;17:484.
[26] Brothers AH, Dunand DC. Acta Mater 2005;53:4427.
[27] Prakash O, Sang H, Embury JD. Mater Sci Eng 1995;A199:195.
[28] Jin I, Kenny LD, Sang H, US Patent No. 5,221,324; 1993.
[29] San Marchi C, Brothers AH, Dunand DC. Mater Res Soc Symp Proc 2003;754:CC1.8.1.
[30] Queheillalt DT, Wadley HNG. Acta Mater 2005;53:303.
[31] Kawamura Y, Kato H, Inoue A, Masumoto T. Appl Phys Lett 1995;67:2008.
[32] Lee PY, Hung SS, Hsieh JT, Lin YL, Lin CK. Intermetallics 2002;10:1277.
[33] Baumgartner F, Duarte I, Banhart J. Adv Eng Mater 2000;2:168.
[34] Dunand DC. Adv Eng Mater 2004;6:369.
[35] Kim HJ, Lee JK, Shin SY, Jeong HG, Kim DH, Bae JC. Intermetallics 2004;12:1109.
[36] Kato H, Kawamura Y, Inoue A, Masumoto T. Mater Sci Eng A 1997;226:458.
[37] Robertson J, Im JT, Karaman I, Hartwig KT, Anderson IE. J Non-Cryst Sol 2003;317:144.
[38] Kim YB, Park HM, Jeung WY, Bae JS. Mater Sci Eng A 2004;368:318.
[39] Kato A, Inoue A, Horikiri H, Masumoto T. Mater Trans JIM 1994;35:125.
[40] Anderson O, Waag U, Schneider L, Stephani G, Kieback B. Adv Eng Mater 2000;2:192.
[41] Szuecs F, Kim CP, Johnson WL. Acta Mater 2001;49:1507.
[42] Fan C, Ott RT, Hufnagel TC. Appl Phys Lett 2002;81:1020.
[43] Wadley HNG, Fleck NA, Evans AG. Compos Sci Technol 2003;63:2331.
[44] Yokoyama Y, Yamano K, Fukaura K, Sunada H, Inoue A. Mater Trans 2001;42:623.
[45] Choi-Yim H, Johnson WL. Appl Phys Lett 1997;71:3808.
[46] Lewandowski JJ, Thurston AK, Lowhaphandu P. 2003 p. 754.
[47] Conner RD, Johnson WL, Paton NE, Nix WD. J Appl Phys 2003;94:904.
[48] Brothers AH, Prine DW, Dunand DC. Intermetallics, in press.
[49] Lund AC, Schuh CA. Intermetallics 2004;12:1159.
[50] Park ES, Kim DH. J Mater Res 2004;19:685.
[51] Inoue A, Negishi T, Kimura HM, Zhang T, Yavari AR. Mater Trans JIM 1998;39:318.
[52] Mudali UK, Baunack S, Eckert J, Schultz L, Gebert A. J Alloy Compd 2004;377:290.
[53] Zander D, Koster U. Mater Sci Eng A 2004;375–77:53.
[54] Parikh SN. Orthopedics 2002;25:1301.
[55] Morrison ML, Buchanan RA, Peker A, Peter WH, Horton JA, Liaw PK. Intermetallics 2004;12:1177.
[56] Hiromoto S, Tsai AP, Sumita M, Hanawa T. Mater Trans 2001;42:656.
[57] Hiromoto S, Numata H, Tsai AP, Nakazawa K, Hanawa T, Sumita M. J Jpn I Met 1999;63:352.
[58] Poitout DG. Biomechanics and biomaterials in orthopedics. New York (NY): Springer; 2004.